Organic & Biomolecular Chemistry

Cite this: *Org. Biomol. Chem.*, 2012, **10**, 8640

www.rsc.org/obc

PAPER

A highly sensitive fluorescent probe based on simple pyrazoline for Zn^{2+} in living neuron cells†

Zhe Zhang,[a] Fang-Wu Wang,[b] Sheng-Qing Wang,[a] Fei Ge,[a] Bao-Xiang Zhao*[a] and Jun-Ying Miao*[b]

Received 17th July 2012, Accepted 10th September 2012
DOI: 10.1039/c2ob26375k

We develop a pyrazoline-based fluorescent sensor for biological Zn^{2+} detection. The sensor shows good binding selectivity for Zn^{2+} over competing metal with 40-fold fluorescence enhancement in response to Zn^{2+}. The new probe is cell-permeable and can be used to detect intracellular zinc ions in living neuron cells.

Introduction

Zinc ion has attracted much attention due to its biological significance. As the second most abundant transition metal ion in the human body after iron, Zn^{2+} shows its vital role in catalytic centers and structural cofactors of many Zn^{2+}-containing enzymes and DNA-binding proteins.[1] It has been reported that zinc plays an essential part in many biological processes, such as brain function and pathology, gene transcription, immune function and mammalian reproduction,[2] as well as some pathological processes, such as Alzheimer's disease, epilepsy, ischemic stroke and infantile diarrhea.[3] Although most Zn^{2+} is tightly bound to enzymes and proteins, free zinc pools exist in some tissues, such as brain, intestine and retina.[4] In addition, while serum zinc levels are low in the setting of most cancers, tumor tissue in breast and lung cancer has elevated zinc levels when compared with the corresponding normal tissues.[5] Zinc deficiency may play an important role in the appearance of diseases, but excess zinc is toxic for the cell. Therefore, the cellular level of zinc must be controlled within a suitable range, which is normally between 0.1 and 0.5 mM.[6] The significance of zinc homeostasis to neuro-physiology and neuropathology has attracted much interest in devising new ways to detect Zn^{2+} in biological samples. Sensitive and selective detection of Zn^{2+} in biological systems, therefore, is essential and strongly desired. In the last decade, numerous scientific endeavors have focused on the development of fluorescent chemosensors for Zn^{2+}, including small molecule,[7] macrocycle[8] and nanoparticles[9] for the *in vitro* and *in vivo* detection of Zn^{2+}. Nevertheless, most of them work in toxic organic-containing solution, which does harm to the biological systems during *in vivo* tests. What is more, their preparation requires complex multistep organic synthesis that costs a lot. Up to now, very few Zn^{2+} probes have been successfully developed for the imaging of Zn^{2+} in neuron cells.[10] Therefore, the development of fluorescent probes with high sensitivity and selectivity for monitoring Zn^{2+} in living neuron cells remains a significant challenge.

Recently, we synthesized a novel fluorescent chemosensor based on pyrazoline and studied the property for detecting zinc ion in the HEPES (20 mM HEPES, pH = 7.2, 50% (v/v) CH_3CN) buffer solution. However, the sensor was limited by the poor turn-on response (3-fold) in the presence of excess Zn^{2+}.[11] Thus, there is a need to develop a new more sensitive probe for Zn^{2+}. In this work, a new approach to developing Zn^{2+} fluorescent sensor based on pyrazoline, 5-(2-(allyloxy)phenyl)-3-(2-hydroxy-5-methylphenyl)-4,5-dihydro-1*H*-pyrazole-1-carbothioamide, is reported. Connected with a group of allyloxy, the lipophilic property of the compound is improved, which gives it the ability to penetrate the membrane easily. Meanwhile, using the thiosemicarbazide to form pyrazoline not only minimizes the steric hindrance compared to using other arylhydrazines, but also adds the group of carbothioamide with more hydrogen bonds in water solution.

Results and discussion

The synthesis of probe **L** (compound **4**) from chalcone (compound **3**) is described in Scheme 1. The structures of **3** and **L** were determined by X-ray analysis (Fig. S1, S2, ESI†). The structure of **L** with 1 equiv. cavities capable of chelating Zn^{2+} possesses a tridentate chelating conformation by the group of phenolic oxygen, pyrazoline N and allyloxy double bond. The formation of **L**–Zn(II) can enhance the immobility of the rotatable bonds, leading to a fairly rigid structure with considerably stronger fluorescence properties than free **L**.

[a]*Institute of Organic Chemistry, School of Chemistry and Chemical Engineering, Shandong University, Jinan 250100, P. R. China. E-mail: bxzhao@sdu.edu.cn*
[b]*Institute of Developmental Biology, School of Life Science, Shandong University, Jinan 250100, P. R. China. E-mail: miaojy@sdu.edu.cn*

†Electronic supplementary information (ESI) available: X-ray crystallographic data of compound **3** and **4**. CCDC 891147 and 891148. For ESI and crystallographic data in CIF or other electronic format see DOI: 10.1039/c2ob26375k

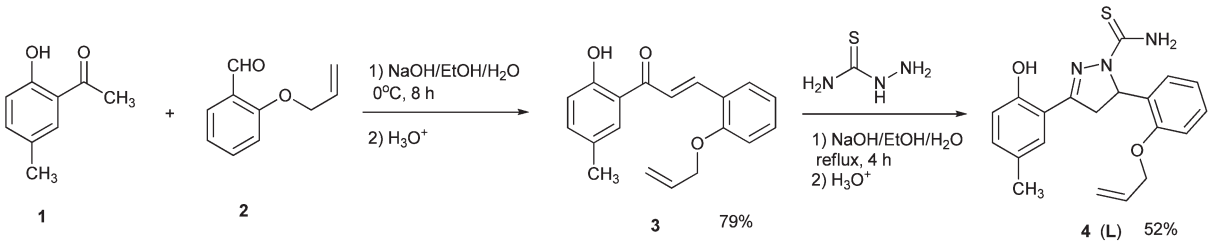

Scheme 1 The synthesis of compound **4** (**L**).

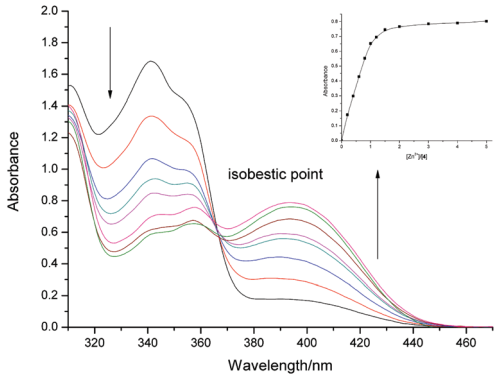

Fig. 1 UV-vis spectra of **L** (100 μM) upon the titration of Zn^{2+} (0.2, 0.4, 0.6, 0.8, 1.0, 1.2, 1.5, 2.0, 3.0, 4.0, 5.0 equiv.) in HEPES buffer solution (20 mM HEPES, pH 7.2, EtOH : H_2O = 1 : 1).

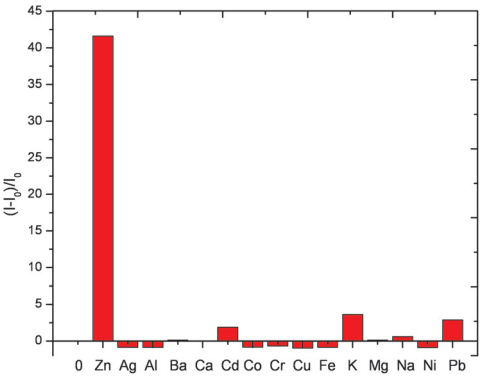

Fig. 2 Fluorescence intensity changes ($(I - I_0)/I_0$) of free **L** (10^{-5} M) at 476 nm in the HEPES buffer solution (20 mM HEPES, pH = 7.2, EtOH : H_2O = 1 : 1) upon addition of various metal ions (10^{-4} M). I and I_0 denote fluorescence intensity of **L** in the presence and absence of metal ions. Excitation wavelength: 395 nm.

To verify the practical applications in a biological environment, the spectroscopic properties of **L** and with different metal ions were measured under simulated physiological conditions (20 mM HEPES buffer at pH 7.2, EtOH : H_2O = 1 : 1). As shown in the ESI (Fig. S3, S4, ESI†), during the UV-vis spectrum of **L** with different concentrations, the absorption maximum is at 341 nm and the ε is 2.5 × 10^4 M^{-1} cm^{-1}. In the UV-vis titration spectra of **L** with Zn^{2+} (0–5 equiv.) (Fig. 1), a decrease of the absorbance at 341 nm and an increase of a new absorption band centered at 395 nm were observed with a distinct isobestic point at 366 nm.

Binding affinities of compound **L** with different metal ions were also evaluated by UV-vis spectroscopy. Upon addition of the metal ions, the absorption spectra vary in different manners, as shown in the ESI (Fig. S5†). In the case of Co^{2+}, Ag^{+}, Cu^{2+}, Ni^{2+}, Hg^{2+} and Zn^{2+}, the addition of the metal ions caused changes in shape. Especially, stronger absorptions appeared in the range of 375–450 nm due to the binding of **L** with Cu^{2+}, Ni^{2+} Co^{2+} and Ag^{+}, whereas the others did not change. The binding of **L** with Cu^{2+}, Ni^{2+} Co^{2+} and Ag^{+} can further quench the fluorescence intensity of **L**.

Ion selectivity is an important property of the fluorescence probes. Thus, we evaluated the fluorescent response of **L** with different metal ions, including Ag^{+}, Ba^{2+}, Ca^{2+}, Cd^{2+}, Co^{2+}, Cr^{3+}, Cu^{2+}, Fe^{3+}, K^{+}, Mg^{2+}, Na^{+}, Ni^{2+} and Pb^{2+} in HEPES buffer solution and found the perfect selectivity for Zn^{2+} with a considerable signal output (Fig. 2). The Job plots were implemented a 1 : 1 stoichiometry for **L**–Zn(II) (Fig. S6, ESI†).

To apply **L** as a probe in a biological environment, determining the tolerance to the interference of physiologically important metal ions in living cells, such as Na^{+}, K^{+} and Ca^{2+}, is necessary. In our research, the concentration of these metal ions were 40 times over Zn^{2+} and showed a negligible effect on the fluorescence response for **L**. The existence of other important transition metal ions may also affect the detection ability of **L**. Iron as the most abundant transition metal ion shows no interference, even in the presence of 10 equiv. iron ions (Fig. S7, ESI†). Compared with some available Zn^{2+} sensors, which exhibit some enhancement of the fluorescence for Cd^{2+},[12] our sensor has a selective response to Zn^{2+} without the interference of Cd^{2+} in the buffered solution, whereas, the existence of copper obviously quenched the fluorescence intensity, which is consistent with previous reports.[7a,13] Thus, this probe can detect Zn^{2+} with minimum interference from other competing metal ions and should have good selectivity for Zn^{2+} in the biological studies. In addition, the intensity of **L**–Zn(II) at 476 nm showed a decrease with the addition of Cu^{2+}, which indicated that Cu^{2+} replaced Zn^{2+} and formed **L**–Cu(II). This property might make it useful as a good ON–OFF sensor for Cu^{2+}.

In the fluorescence titration spectra of **L** with Zn^{2+} (0–50 equiv.) excited at 395 nm (Fig. 3), **L** alone shows a weak fluorescence emission band at 476 nm with a quite weak fluorescence quantum yield (0.0023). When adding the Zn^{2+} to the buffer solution, a gradual increase in fluorescence (fluorescence quantum yield 0.091) with a conspicuous color change from colorless to yellow is found. From the photo in the ESI (Fig. S8†), we can see the stronger blue emission of **L** with addition of 10 μM Zn^{2+} ion under the irradiation at 365 nm than without the addition of

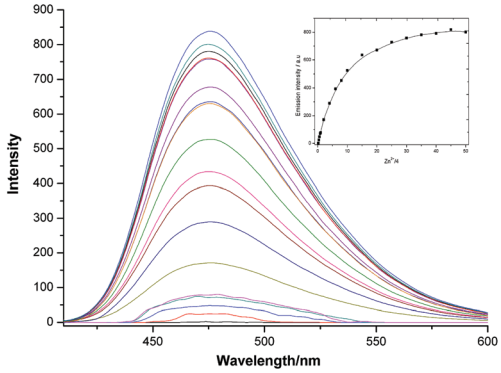

Fig. 3 Fluorescence emission spectra of **L** (10^{-5} M) was titrated with Zn^{2+} (0–50 × 10^{-5} M) in the HEPES buffer solution (20 mM HEPES, pH = 7.2, EtOH : H_2O = 1 : 1). Inset: changes of fluorescence intensity of **L** (10^{-5} M) with different equivalents of Zn^{2+} at 476 nm.

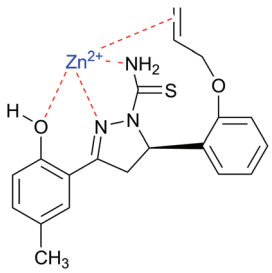

Fig. 4 The proposed binding mode of **L** with Zn^{2+} in aqueous solution.

Zn^{2+} ion, presumably due to the blocking of the photoinduced electron transfer (PET) process upon complexation with Zn^{2+}. The fluorescence enhancement was approximately 40-fold in the presence of excess Zn^{2+}.

A proposed binding mode is shown in Fig. 4. The fact that the hydrogens bound to the double bond of the allyloxy group were disordered by X-ray analysis indicated that the π-electrons were delocalized. The interactions of delocalized π-electron systems with metal centers are of fundamental importance in organometallic chemistry and have received considerable attention. The allyl group represents the simplest delocalized π-electron system and allyl metal complexes are therefore ideal model systems.[14] To get an insight into the binding mode, ^{1}H NMR titration experiments were also performed. Fig. S9† in the ESI shows the change in ^{1}H NMR of **L** in the absence and presence of 0.2 equiv. Zn^{2+}. As a result of metal chelation, all protons in the allyl and aryl groups showed an upfield or downfield shift, which are attributed to the changes in electron density. The double bond in the allyloxy moiety as a ligand contributes an electron to a zinc orbital.

Following a Benesi–Hildebrand-type analysis,[15] the association constant K_a was determined to be 4.83 × 10^4 M^{-1}. The fluorescent titration profile of **L** with Zn^{2+} demonstrated that the detection limit of Zn^{2+} is 6.1 × 10^{-7} M (Fig. S10, ESI†).

For practical application, the appropriate pH conditions for successful operation of the probe were explored. It is interesting to observe the bell-shaped profile (Fig. S11, ESI†). The structure

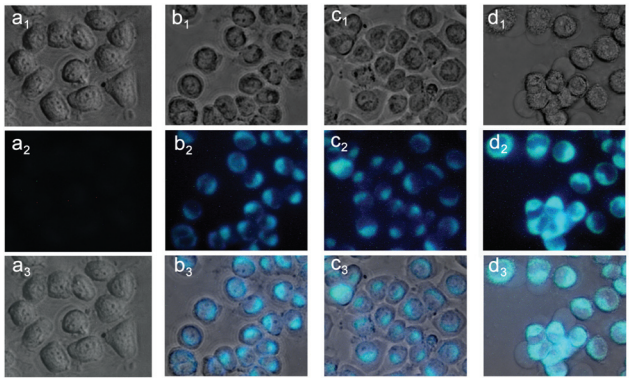

Fig. 5 Fluorescence microscope images of living PC12 cells. (a_1–a_3): images of cells incubated with 10 μM probe **L** for 30 min at 37 °C. Cells were exposed to pyrithione (pyr, concentration equivalent of 1/2 added Zn^{2+}) in the presence of increased concentrations of extracellular Zn^{2+} as (b_1–b_3) 10, (c_1–c_3) 25 and (d_1–d_3) 50 μM following incubation with probe **L** for 30 min. (a_1–d_1) Bright-field, (a_2–d_2) fluorescent, (a_3–d_3) overlay image. Scale bar = 10 μm.

of **L** contains a phenol hydroxyl with acidity and a nitrogen atom with basicity. In the condition of strong acidity, nitrogen might be protonated to suppress the binding ability to Zn(II), so that the fluorescence decreases. Whereas, when pH > 11, hydroxyl in phenol may undergo deprotonation, which might influence the binding model to lower fluorescence. The strong and stable fluorescence of **L**–Zn(II) in the biologically relevant pH range indicated its practicality in physiological conditions.

The intracellular Zn^{2+} imaging behaviour of **L** was studied on PC12 neuronal cells by a fluorescence microscope. After incubation with DMSO-containing **L** (10 μM, DMSO : water = 1 : 100) for 30 min at 37 °C, the cells exhibited very faint fluorescence. However, fluorescence became clearly visible in the cytoplasm of PC12 cells when exogenous Zn^{2+} was introduced into the cells in the presence of a zinc-selective ionophore, pyrithione (2-mercaptopyridine *N*-oxide), providing visual evidence of the probe **L** readily entering cells and information on the intracellular existence of Zn^{2+} (Fig. 5). Moreover, with increasing concentration of Zn^{2+} incubated, the fluorescence intensity enhanced obviously in a concentration-dependent manner. These results demonstrate that probe **L** has the potential for biological applications.

Conclusions

In summary, a new fluorescent sensor for Zn^{2+} has been designed and synthesized by taking advantage of the pyrazoline derivative. This sensor exhibits good sensitivity and selectivity toward Zn^{2+} in aqueous solution. Moreover, the sensor can monitor intracellular Zn^{2+} level in living neuronal cells.

Experimental section

Materials and characterization

Deionized water was used throughout the experiment of absorption and fluorescence determination. All of the reagents were

purchased from commercial suppliers and used without further purification. The solutions of metal ions were prepared from $NaNO_3$, $Mg(NO_3)_2{\cdot}6H_2O$, $Al(NO_3)_3{\cdot}9H_2O$, KNO_3, $Ca(NO_3)_2{\cdot}4H_2O$, $Cr(NO_3)_3{\cdot}9H_2O$, $Fe(NO_3)_3{\cdot}9H_2O$, $Co(NO_3)_2{\cdot}6H_2O$, $Ni(NO_3)_2{\cdot}6H_2O$, $Cu(NO_3)_2{\cdot}3H_2O$, $Zn(NO_3)_2{\cdot}6H_2O$, $AgNO_3$, $Cd(NO_3)_2{\cdot}4H_2O$, $Ba(NO_3)_2$ and $Pb(NO_3)_2$ with deionized water. All samples were prepared at room temperature, shaken for 10 s and left to stand for 18 h before UV-vis and fluorescence determination. Thin-layer chromatography (TLC) was conducted on silica gel 60 F_{254} plates (Merck KGaA). HEPES buffer solutions (pH 7.2) were prepared using 20 mM HEPES and the appropriate amount of aqueous sodium hydroxide using a pH meter. ^{1}H NMR (300 MHz) and ^{13}C NMR (75 MHz) spectra were recorded on a Bruker Avance 300 spectrometer using $CDCl_3$ as the solvent and tetramethylsilane (TMS) as the internal standard. Melting points were determined on a XD-4 digital micro melting point apparatus. IR spectra were recorded with an IR spectrophotometer VERTEX 70 FT-IR (Bruker Optics). HRMS spectra were recorded on a Q-TOF6510 spectrograph (Agilent). UV-vis spectra were recorded on a U-4100 UV-Vis-NIR Spectrometer (Hitachi). Fluorescent measurements were recorded on a Hitachi F-4500 fluorescence spectrophotometer.

Cell culture and imaging

PC12 cells were grown in Dulbecco's Modified Eagle's Medium (DMEM, Gibco), containing 10% fetal bovine serum (Gibco), 5% donor horse serum (Biological Industries) and 1% PSN antibiotic, at 37 °C in a humidified incubator with 5% CO_2. For the experimental study, cells were grown to 80–90% confluence, harvested with 0.05% trypsin (Sangon Biotech) in phosphate-buffered saline (PBS) and plated at the desired cell concentration. For fluorescence imaging, the cells were seeded into 24-well plates and experiments to assay Zn^{2+} uptake were performed in the same media supplemented with different concentrations of zinc nitrate with pyrithione (zinc ionophore, concentration equivalent of 1/2 added Zn^{2+}). The cells were rinsed twice with PBS and treated with DMSO-containing **L** (10 μM, DMSO : water = 1 : 100) for 30 min at 37 °C. After washing twice with PBS, the cells were imaged under an inverted fluorescence microscope (Nikon TE2000-S).

Synthesis of (*E*)-3-(2-(allyloxy)phenyl)-1-(2-hydroxy-5-methylphenyl)prop-2-en-1-one (3)

Chalcone **3** was easily prepared from compound **1** and **2** in 78.8% yield. Yellow solid, mp: 166–167 °C. ^{1}H NMR (300 MHz, $CDCl_3$): 2.34 (s, 3H, CH_3), 4.67 (dt, 2H, J = 5.4, 1.5 Hz, CH_2 in the allyloxy moiety), 5.36 (dd, 1H, J_{ABcis} = 9, J_{BC} = 1.5 Hz, =CH*H*), 5.50 (dd, 1H, $J_{ACtrans}$ = 19, J_{BC} = 1.5 Hz, =C*H*H), 6.10–6.23 (m, 1H, =CH–), 6.93 (d, 1H, J = 8.4 Hz, ArH), 6.95 (t, 1H, J = 8.7 Hz, ArH), 7.31 (d, 1H, J = 8.4 Hz, ArH), 7.38 (t, 1H, J = 8.4 Hz, ArH), 7.65 (d, 1H, J = 8.4 Hz, ArH), 7.69 (s, 1H, ArH), 7.87 (d, 1H, J_{trans} = 15.6 Hz, =CH–, conjugated vinyl), 8.19 (d, 1H, J_{trans} = 15.6 Hz, =CH–, conjugated vinyl), 12.75 (s, 1H, OH). The structure of compound **3** was also determined by X-ray analysis and is shown in Fig. S1† (CCDC no. 891148).

Synthesis of 5-(2-(allyloxy)phenyl)-3-(2-hydroxy-5-methylphenyl)-4,5-dihydro-1*H*-pyrazole-1-carbothioamide (4)

Compound **4** was prepared by the reaction of chalcone (**3**) and thiosemicarbazide. Briefly, NaOH and thiosemicarbazide was added to a stirred solution of chalcone (**3**) in ethanol and refluxed for 4 h (monitored by TLC). After reaction, the mixture was cooled to room temperature and hydrochloric acid was added in droplets to neutralize it to pH 7. The crude product was obtained as a yellow solid, which was recrystallized from ethanol to obtain compound **4**. White solid; yield: 52%; mp: 222–223 °C; IR (KBr, cm^{-1}): 3436.6, 3326.8, 1600.4, 1481.1, 1337.7, 1250.9, 816.8, 746.7; ^{1}H NMR (300 MHz, $CDCl_3$): 2.27 (s, 3H, CH_3), 3.25 (dd, 1H, J = 18, 3.6 Hz, CH*H* in pyrazoline moiety), 3.90 (dd, 1H, J = 18, 11.4 Hz, C*H*H in pyrazoline moiety), 4.57 (d, 2H, J = 5.4 Hz, CH_2 in allyloxy moiety), 5.23 (d, 1H, J_{ABcis} = 10.5 Hz, =CH*H*), 5.37 (d, 1H, $J_{ACtrans}$ = 17.1, =C*H*H), 5.93–6.06 (m, 1H, =CH–), 6.24 (dd, 1H, J = 11.4, 3.6 Hz, CH in pyrazoline moiety), 6.26–6.60 (m, 2H, NH_2), 6.88–6.96 (m, 3H, Ar–H), 7.00 (s, 1H, Ar–H), 7.09–7.26 (m, 3H, Ar–H), 9.53 (s, 1H, OH); ^{13}C NMR (75 MHz, $CDCl_3$): 175.7, 159.2, 155.0, 154.5, 133.2, 132.4, 128.7, 128.5, 128.4, 128.1, 126.4, 120.3, 117.2, 116.3, 114.0, 111.8, 68.6, 58.5, 41.8, 19.9; HRMS: calcd for $[M + H]^+$ $C_{20}H_{22}N_3O_2S$: 368.1433; found: 368.1424. The X-ray structure is shown in Fig. S2† (CCDC no. 891147).

Acknowledgements

This study was supported by 973 Program (2010CB933504) and National Natural Science Foundation of China (90813022 and 20972088).

Notes and references

1 (*a*) X. Xie and T. G. Smart, *Nature*, 1991, **349**, 521; (*b*) C. E. Outten and T. V. O'Halloran, *Science*, 2001, **292**, 2488; (*c*) L. A. Finney and T. V. O'Halloran, *Science*, 2003, **300**, 931.
2 (*a*) B. L. Vallee and K. H. Falchuk, *Physiol. Rev.*, 1993, **73**, 79; (*b*) J. M. Berg and Y. Shi, *Science*, 1996, **271**, 1081.
3 (*a*) C. J. Frederickson, M. D. Hernandez and J. F. McGinty, *Brain Res.*, 1989, **480**, 317; (*b*) A. I. Bush, W. H. Pettingell, G. Multhaup, M. Paradis, J. P. Vonsattel, J. F. Gusella, K. Beyreuther, C. L. Masters and R. E. Tanzi, *Science*, 1994, **265**, 1464; (*c*) A. I. Bush, W. H. Pettingell, M. D. Paradis and R. E. Tanzi, *J. Biol. Chem.*, 1994, **269**, 12152; (*d*) L. C. Costello, Y. Liu, J. Zou and R. B. Franklin, *J. Biol. Chem.*, 1999, **274**, 17499.
4 (*a*) A. Takeda, *BioMetals*, 2001, **14**, 343; (*b*) W. J. Qian, K. R. Gee and R. T. Kennedy, *Anal. Chem.*, 2003, **75**, 3468; (*c*) C. J. Frederickson, J. Y. Koh and A. I. Bush, *Nat. Rev. Neurosci.*, 2005, **6**, 449.
5 E. J. Margalioth, J. G. Schenker and M. Chevion, *Cancer Sci.*, 1983, **52**, 868.
6 D. J. Eide, *Biochim. Biophys. Acta*, 2006, **1763**, 711.
7 (*a*) N. Y. Baek, C. H. Heo, C. S. Lim, G. Masanta, B. R. Cho and H. M. Kim, *Chem. Commun.*, 2012, **48**, 4546; (*b*) Z. Xu, X. Liu, J. Pan and D. R. Spring, *Chem. Commun.*, 2012, **48**, 4764; (*c*) L. Xue, G. Li, C. Yu and H. Jiang, *Chem.–Eur. J.*, 2012, **18**, 1050; (*d*) Y. Zhou, Z. X. Li, S. Q. Zang, Y. Y. Zhu, H. Y. Zhang, H. W. Hou and T. C. Mak, *Org. Lett.*, 2012, **14**, 1214; (*e*) F. Sun, G. Zhang, D. Zhang, L. Xue and

H. Jiang, *Org. Lett.*, 2011, **13**, 6378; (*f*) S. Lee, J. H. Lee, T. Pradhan, C. S. Lim, B. R. Cho, S. Bhuniya, S. Kim and J. S. Kim, *Sens. Actuators, B*, 2011, **160**, 1489; (*g*) U. C. Saha, B. Chattopadhyay, K. Dhara, S. K. Mandal, S. Sarkar, A. R. Khuda-Bukhsh, M. Mukherjee, M. Helliwell and P. Chattopadhyay, *Inorg. Chem.*, 2011, **50**, 1213; (*h*) K. Hanaoka, Y. Muramatsu, Y. Urano, T. Terai and T. Nagano, *Chem.–Eur. J.*, 2010, **16**, 568; (*i*) P. Du and S. J. Lippard, *Inorg. Chem.*, 2010, **49**, 10753; (*j*) Y. Zhou, H. N. Kim and J. Yoon, *Bioorg. Med. Chem. Lett.*, 2010, **20**, 125; (*k*) F. Qian, C. Zhang, Y. Zhang, W. He, X. Gao, P. Hu and Z. Guo, *J. Am. Chem. Soc.*, 2009, **131**, 1460; (*l*) Z. Liu, C. Zhang, Y. Li, Z. Wu, F. Qian, X. Yang, W. He, X. Gao and Z. Guo, *Org. Lett.*, 2009, **11**, 795; (*m*) T. Mistri, M. Dolai, D. Chakraborty, A. R. Khuda-Bukhsh, K. K. Das and M. Ali, *Org. Biomol. Chem.*, 2012, **10**, 2380; (*n*) G. Q. Xie, Y. J. Shi, F. P. Hou, H. Y. Liu, L. Huang, P. X. Xi, F. J. Chen and Z. Z. Zeng, *Eur. J. Inorg. Chem.*, 2012 (2), 327.

8 (*a*) C. E. Felton, L. P. Harding, J. E. Jones, B. M. Kariuki, S. J. Pope and C. R. Rice, *Chem. Commun.*, 2008 (46), 6185; (*b*) Y. Fu, Z. T. Xing, C. C. Zhu, H. W. Yang, W. J. He, C. J. Zhu and Y. X. Cheng, *Tetrahedron Lett.*, 2012, **53**, 804; (*c*) D. Buccella, J. A. Horowitz and S. J. Lippard, *J. Am. Chem. Soc.*, 2011, **133**, 4101.

9 G. Kang, H. J. Son, J. M. Lim, H. S. Kweon, I. S. Lee, D. M. Kang and J. H. Jung, *Chem.–Eur. J.*, 2012, **18**, 5843.

10 (*a*) K. Komatsu, Y. Urano, H. Kojima and T. Nagano, *J. Am. Chem. Soc.*, 2007, **129**, 13447; (*b*) E. M. Nolan, J. W. Ryu, J. Jaworski, R. P. Feazell, M. Sheng and S. J. Lippard, *J. Am. Chem. Soc.*, 2006, **128**, 15517; (*c*) L. Kiedrowski, *J. Neurochem.*, 2012, **121**, 438; (*d*) E. M. Nolan and S. J. Lippard, *Acc. Chem. Res.*, 2009, **42**, 193.

11 Z. L. Gong and B. X. Zhao, *Sens. Actuators, B*, 2011, **159**, 148.

12 X. M. Meng, S. X. Wang, Y. M. Li, M. Z. Zhu and Q. X. Guo, *Chem. Commun.*, 2012, **48**, 4196.

13 E. U. Akkaya, M. E. Huston and A. W. Czarnik, *J. Am. Chem. Soc.*, 1990, **112**, 3590.

14 C. Lichtenberg, J. Engel, T. P. Spaniol, U. Englert, G. Raabe and J. Okuda, *J. Am. Chem. Soc.*, 2012, **134**, 9805.

15 M. J. Yuan, W. D. Zhou, X. F. Liu, M. Zhu, J. B. Li, X. D. Yin, H. Y. Zheng, Z. C. Zuo, C. B. Ouyang, H. B. Liu, Y. L. Li and D. B. Zhu, *J. Org. Chem.*, 2008, **73**, 5008.

